Open Access



Asian Journal of Environmental Research
E-ISSN: 3047-4930
DOI: https://doi.org/10.69930/ajer.v3i3.984
Research Article

ScienceTech Group

Vol. 3 (3), 2026
Page: 352-365

Assessment of Tsunami Inundation Expansion Under Multi-Run-up Scenarios Using GIS-Based Spatial Modeling in Gadingsari Coastal Area, Bantul, Indonesia

Ummu Salma *, Stefanie Jessica Henny Larasati

Departement of Marine Science, Faculty of Fisheries and Marine Science, Universitas Diponegoro, Indonesia
*Email (corresponding author): ummusalma@lecturer.undip.ac.id

Abstract. *The southern coastal area of Bantul Regency, Indonesia, is a vulnerable region exposed to tsunami hazards generated by tectonic activity along the southern Java subduction zone. Understanding the spatial characteristics of tsunami inundation under different wave height scenarios is essential to support hazard assessment and coastal mitigation planning. This study aims to analyze the spatial expansion of tsunami inundation under multiple run-up scenarios and evaluate the relationship between inundation patterns and local topographic characteristics in the Gadingsari coastal area. A Geographic Information System (GIS)-based approach was applied by integrating Digital Elevation Model (DEM), slope, and land-use data as spatial parameters. Tsunami propagation was simulated using the energy loss approach (Hloss) combined with surface roughness coefficients and terrain slope analysis through Cost Distance modeling. Three tsunami run-up scenarios were evaluated, namely 10 m, 15 m, and 20 m. The results show that increasing tsunami height significantly expands the inundation extent, with affected areas of 4.436 ha, 6.716 ha, and 9.264 ha for the 10 m, 15 m, and 20 m scenarios, respectively. The transition from the 10 m to 20 m scenario increased the modeled inundation area by 4.829 ha (108.85%), based on the unrounded GIS-derived area values. The inundated areas were mainly distributed within elevation classes of 7.5–10 m and slope classes of 2–5°. The remaining tsunami height distribution showed similar spatial patterns across all scenarios. These findings demonstrate that GIS-based multi-scenario modeling can effectively describe tsunami inundation variability and provide spatial information to support tsunami risk evaluation and mitigation planning in coastal areas.*

Keywords: *Tsunami Inundation; Geographic Information System (GIS); Tsunami Run-Up; Cost Distance; Hloss*

1. Introduction

Tsunamis are among the most destructive coastal hazards, capable of causing extensive impacts on coastal populations, infrastructure, and economic activities. Indonesia is particularly exposed to tsunami hazards because of its complex tectonic setting, including the active Sunda subduction zone where the Indo-Australian Plate converges with and subducts beneath the Sunda/Eurasian margin (1,2). The southern coast of Java is recognized as one of the regions with considerable tsunami potential, as megathrust earthquakes along the Java subduction zone can generate large tsunami waves affecting densely populated coastal areas (1,2). Therefore, accurate assessment of tsunami hazard characteristics, particularly tsunami inundation extent, is essential to support disaster risk reduction and coastal management.

Tsunami inundation is controlled by complex interactions between tsunami characteristics and coastal environmental conditions. Although tsunami wave height is a

Received: 6 October 2026 / Accepted: 9 November 2026 / Available online:19 November 2026

primary factor determining coastal impacts, inland propagation is also strongly influenced by topographic and surface characteristics, including elevation, slope, land cover, and surface roughness (3,4). Low-elevation coastal areas with gentle slopes and relatively low surface roughness generally facilitate farther inland propagation, whereas vegetation, buildings, and other rough surfaces can increase flow resistance and modify tsunami inundation characteristics (4,5). Consequently, tsunami hazard assessment requires spatial approaches capable of integrating multiple environmental parameters to describe variations in tsunami inundation.

Various approaches have been developed to estimate tsunami inundation, ranging from comprehensive hydrodynamic simulations to simplified spatial and energy-loss models. Physics-based numerical models can provide detailed information on tsunami propagation and inundation dynamics; however, high-resolution simulations may require substantial topographic data and computational resources (6). Alternatively, Geographic Information System (GIS)-based approaches provide a practical framework for integrating elevation, slope, land-use, surface-roughness, and tsunami-height information to estimate potential inundation areas (5,7). Recent GIS-based studies in Indonesia have demonstrated the use of Digital Elevation Model (DEM) data, land-cover-derived roughness coefficients, terrain slope, and Cost Distance analysis for tsunami inundation mapping (5,7). The Hloss approach, originally based on tsunami-height attenuation associated with terrain slope and surface roughness, can be integrated with Cost Distance analysis to represent progressive tsunami energy loss during inland propagation (7,8).

The southern coastal area of Bantul Regency, including the Gadingsari coastal region, is situated along a tsunami-prone section of southern Java. Previous studies in Bantul have applied both GIS-based inundation modeling and numerical tsunami simulations using topographic data to evaluate potential tsunami impacts and support evacuation planning (7, 9). Building on these studies, the present research focuses on how different tsunami run-up scenarios alter inundation extent, inland penetration, and the spatial distribution of remaining tsunami height at a local scale. Evaluating these spatial variations is important because changes in initial tsunami height, together with local terrain and surface conditions, can produce different patterns of inland inundation.

This study aims to assess the spatial expansion of tsunami inundation under multiple run-up scenarios in the Gadingsari coastal area, Bantul Regency, using a GIS-based spatial modeling approach. Three tsunami run-up scenarios (10 m, 15 m, and 20 m) were evaluated to analyze changes in inundation extent, inland penetration distance, elevation characteristics, slope distribution, and remaining tsunami height patterns. The findings provide spatial information regarding tsunami impact variability and contribute to improving tsunami hazard assessment and mitigation planning in coastal regions. The scenario-based inundation maps may also provide a spatial basis for environmentally informed coastal planning by identifying areas where coastal vegetation, agricultural land, and other environmentally sensitive zones may become exposed under higher run-up conditions. Such information can support the integration of disaster-risk reduction with sustainable land-use planning and coastal ecosystem management.

2. Methods

2.1. Study Area

The study was conducted in the Gadingsari coastal area, Bantul Regency, Special Region of Yogyakarta, Indonesia. The study area is located along the southern coast of Java, which is exposed to potential tsunami hazards associated with seismic activity along the Java subduction zone. Previous tsunami inundation modeling in Bantul Regency has identified the southern coastal area as potentially exposed under multiple run-up scenarios (7). The analysis area covers the coastal zone extending from the shoreline toward inland areas to evaluate tsunami propagation and inundation characteristics. All spatial analyses were performed using the WGS 1984 Universal Transverse Mercator (UTM) Zone 49S coordinate system.

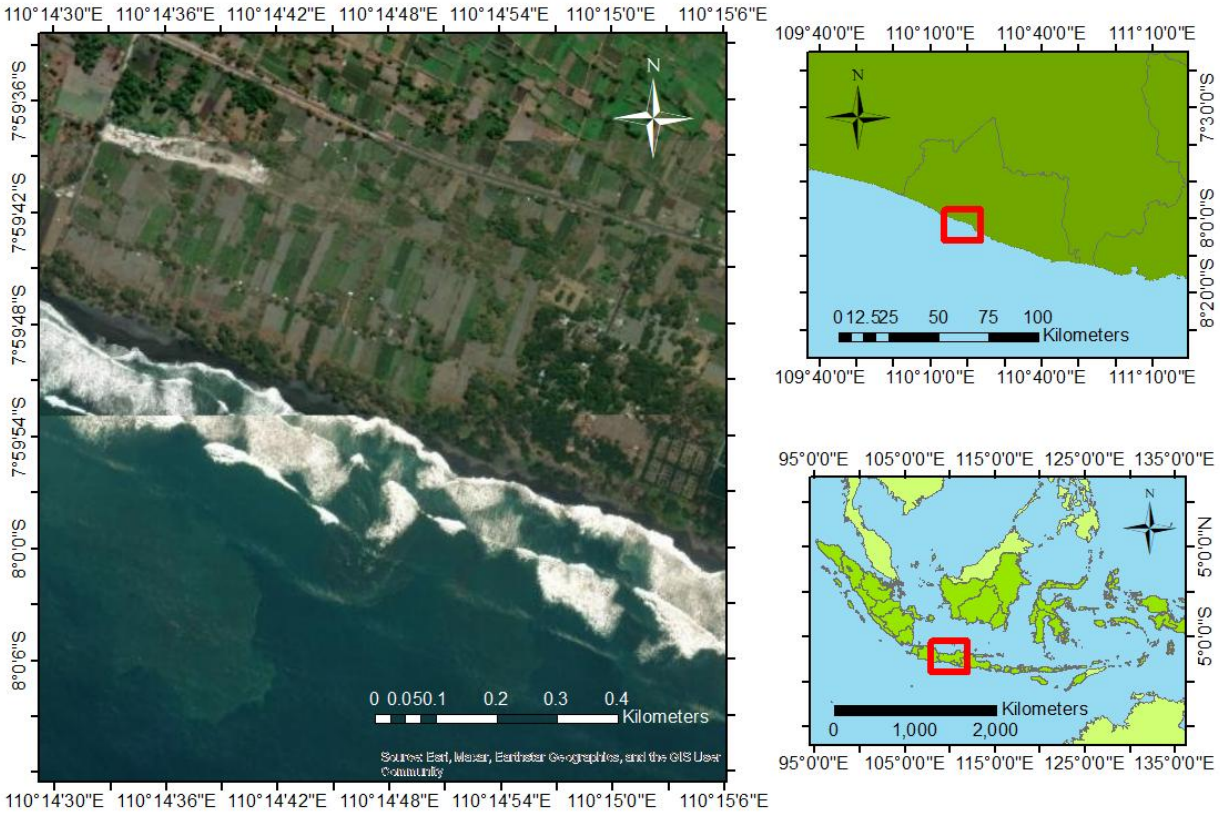


Figure 1. Location map of the study area in the Gadingsari coastal region, Bantul Regency, Indonesia.

2.2. Data Sources and Pre-processing

This study utilized spatial datasets consisting of topographic, coastal, and land-use information. Digital Elevation Model (DEM) data were obtained from the National Digital Elevation Model (DEMNAS), provided by the Geospatial Information Agency of Indonesia (Badan Informasi Geospasial/BIG). DEMNAS has a native spatial resolution of 0.27 arc-second and uses the EGM2008 vertical datum. The DEM tiles covering the study area were mosaicked, projected to WGS 1984 UTM Zone 49S, and clipped to the study-area boundary. The raster cell size used for subsequent slope and Cost Distance analyses was 8 m. The official DEMNAS service is maintained by BIG and provides national elevation data for Indonesia (10).

Coastline and land-use datasets were obtained from the Ina-Geoportal (TanahAir Indonesia), maintained by BIG. The coastline dataset was used to define the initial source boundary for tsunami propagation, whereas land-use data were used to assign surface roughness coefficients representing differences in resistance to tsunami flow. The coastline was buffered by 8 m and converted to a raster to define the initial tsunami source zone. The resulting source raster was aligned with the analysis grid and used as the source input in the Cost Distance analysis. Ina-Geoportal serves as Indonesia's national platform for sharing geospatial datasets from government institutions (11).

All spatial data processing was conducted using ArcGIS 10.8 with the Spatial Analyst extension. Pre-processing included coordinate-system standardization, DEM mosaic processing, raster projection, and clipping to the study-area boundary. A slope raster was subsequently derived from the DEM to represent terrain inclination. Prior to trigonometric calculation, slope values expressed in degrees were converted to radians because the ArcGIS trigonometric functions interpret input values in radians.

2.3. Surface Roughness Classification

Surface roughness was incorporated into the inundation model to represent differences in resistance to tsunami propagation among land-use/land-cover types. Each land-use class was assigned a surface roughness coefficient (n) following coefficient values used in previous GIS-based tsunami inundation studies employing the Berryman approach (5,8). The coefficients applied in this study are presented in Table 1.

Table 1. Surface roughness coefficients assigned to land-use/land-cover classes used in the tsunami inundation model.

Land-use/Land-cover type	Roughness coefficient (n)
Water body	0.007
Bush/Shrub	0.040
Forest	0.070
Plantation	0.035
Bare/Open land	0.015
Agricultural land	0.025
Settlement/Built-up area	0.045
Mangrove	0.025
Pond	0.010

2.4. Tsunami Inundation Modeling

Tsunami inundation was modeled using a GIS-based spatial approach integrating terrain slope, land-use-derived surface roughness, and tsunami run-up height. The approach followed the empirical inundation model described by Berryman (2005), in which tsunami height loss during inland propagation is estimated from surface roughness and terrain slope (8).

The tsunami height loss per unit inland propagation distance was calculated as:

$$H_{loss} = \frac{167n^2}{H_0^{1/3}} + 5sin(S) \quad (1)$$

where:

H_{loss} = tsunami height loss per metre of inland propagation (m m^{-1});

n = Manning roughness coefficient representing surface resistance;

H_0 = prescribed tsunami height at the coastline (m); and

S = terrain slope

Terrain slope was initially derived from the DEM in degrees. Because the ArcGIS trigonometric function requires angular values in radians, slope values were converted prior to application of the sine term using $S_{rad} = S_{deg} \times \pi/180$. The resulting H_{loss} raster represents the spatially varying rate of tsunami-height reduction associated with surface roughness and terrain slope.

Three tsunami run-up scenarios were evaluated: 10 m, 15 m, and 20 m. The use of these scenarios is consistent with previous inundation modeling conducted for Bantul Regency using the Berryman-based GIS approach (7).

2.5. Cost Distance Analysis and Remaining Tsunami Height Estimation

For each run-up scenario, the H_{loss} values were calculated on a cell-by-cell basis using the corresponding initial tsunami height, terrain slope, and land-use-derived Manning roughness coefficient. The resulting H_{loss} raster was used as the cost surface in the ArcGIS Cost Distance analysis, while the shoreline-derived raster was specified as the source. Cost Distance accumulated the spatially varying tsunami-height loss along the inland propagation pathway from the coastline. The accumulated cost therefore represents cumulative tsunami-height attenuation rather than the local H_{loss} value of an individual raster cell (7,8).

Three separate simulations were performed using initial tsunami heights of 10, 15, and 20 m. All input rasters were processed using the same coordinate system, spatial extent, and cell size of 8 m to maintain spatial consistency among scenarios.

The remaining tsunami height was calculated using:

$$H_{remain} = H_0 - H_{loss} \quad (2)$$

where:

H_{remain} = remaining tsunami height after inland propagation (m);

H_0 = initial tsunami height at the coastline (m); and

H_{loss} = cumulative tsunami-height loss obtained from the Cost Distance analysis (m)

Areas with H_{remain}>0 were classified as tsunami inundation areas, whereas cells with H_{remain}>0 were classified as non-inundated.

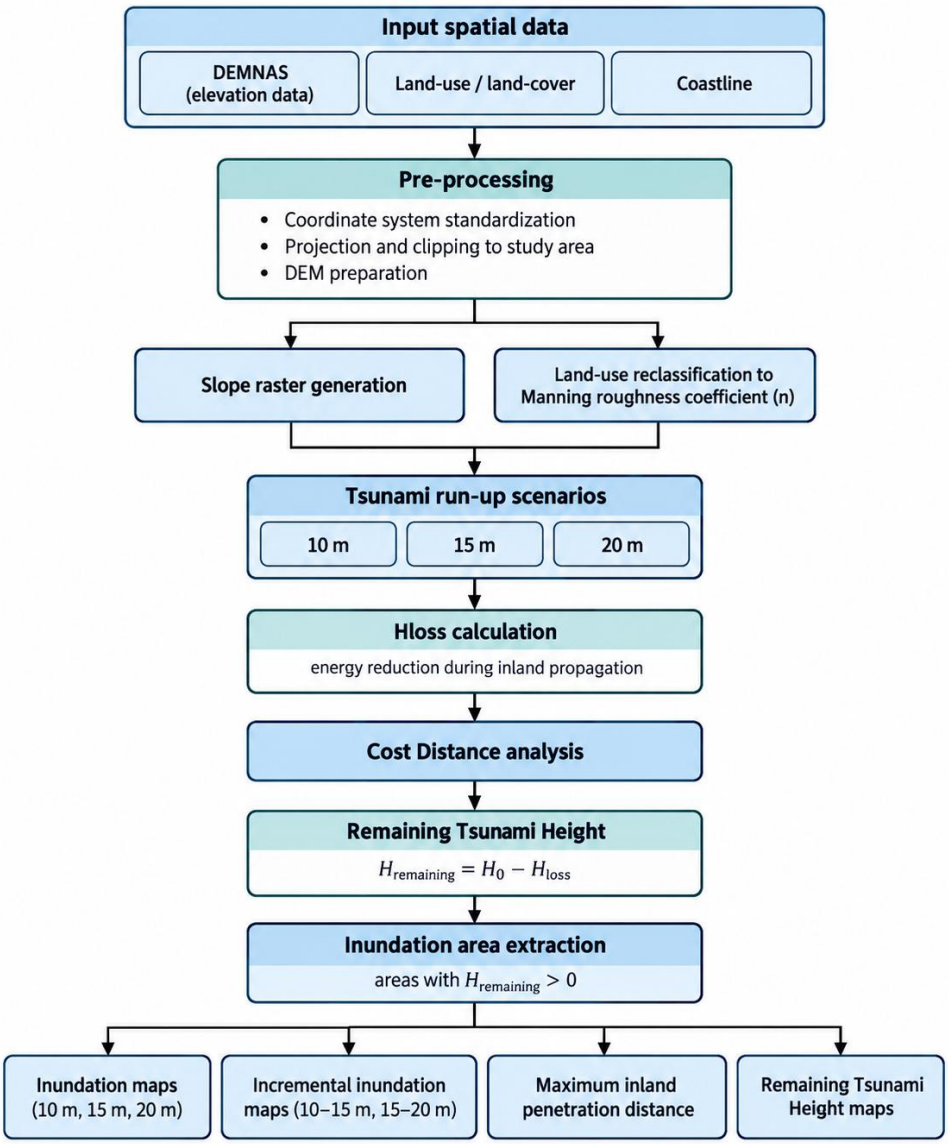


Figure 2. Workflow of GIS-based tsunami inundation modeling.

2.6. Model Evaluation

The modeled inundation boundaries were qualitatively compared with the tsunami evacuation-zone information issued by Badan Penanggulangan Bencana Daerah Kabupaten Bantul in 2023 for the Gadingsari coastal area. The comparison focused on the spatial correspondence between the modeled inundation extent and the existing evacuation-zone boundary. No pixel-based accuracy assessment, goodness-of-fit statistic, or quantitative validation against observed tsunami inundation was performed because observed inundation data for the modeled scenarios were not available. Therefore, this comparison was used only as a qualitative consistency check and should not be interpreted as formal validation of model accuracy.

3. Results and Discussion

3.1. Expansion of Tsunami Inundation under Different Run-up Scenarios

The GIS-based model produced distinct inundation patterns under the three tsunami run-up scenarios of 10, 15, and 20 m (Figure 3). The modeled inundation area increased progressively from 4.436 ha under the 10 m scenario to 6.716 ha under the 15 m scenario and

9.264 ha under the 20 m scenario (Table 2). Relative to the 10 m scenario, the inundated area increased by approximately 51.4% at 15 m and by 108.85% at 20 m. All area differences and percentage changes were calculated from the unrounded GIS outputs (4.435924, 6.715878, and 9.264468 ha for the 10, 15, and 20 m scenarios, respectively), whereas values presented in the tables were rounded to three decimal places. Consequently, direct subtraction of the rounded values may result in a 0.001 ha difference.

A similar relationship between tsunami height and inundation extent has been reported in previous GIS-based assessments along the southern coast of Java. In Bantul Regency, Budiman et al. (7) applied 10, 15, and 20 m run-up scenarios using a GIS-based inundation approach and also observed a progressive increase in inundated area with increasing run-up height. Likewise, Arrisaldi et al. (5) reported substantial expansion of modeled hazard zones at Sawarna Beach as the simulated tsunami height increased. Although the absolute inundation areas cannot be directly compared because of differences in study-area extent, topography, spatial resolution, and model configuration, the consistent trend supports the sensitivity of coastal inundation extent to the initial tsunami-height scenario.

Within the attenuation-based framework used in the present study, a greater initial tsunami height allows a positive remaining tsunami height to persist over a longer inland pathway before being reduced by terrain slope and surface resistance. Consequently, the 20 m scenario reached areas that remained outside the modeled inundation boundary under the lower scenarios. This relationship should, however, be interpreted as a model response to prescribed run-up scenarios rather than as a prediction of the probability of a specific future tsunami event.

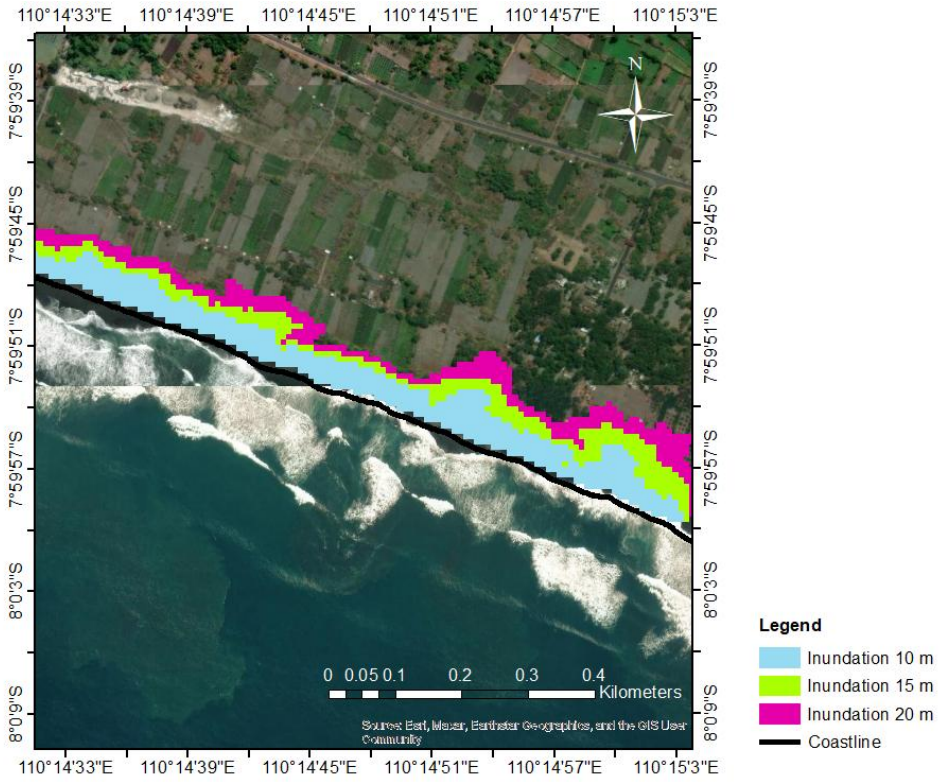


Figure 3. Spatial distribution of modeled tsunami inundation under the 10 m, 15 m, and 20 m run-up scenarios.

Table 2. Inundation area under different tsunami run-up scenarios.

Tsunami scenario	Inundation area (ha)
10 m	4.436
15 m	6.716
20 m	9.264

3.2. Spatial Expansion Pattern between Tsunami Scenarios

Incremental analysis showed that the expansion of inundation was not identical between consecutive scenarios. Increasing the run-up height from 10 to 15 m resulted in an additional inundated area of 2.280 ha, corresponding to approximately 51.4% of the 10 m inundation area. A further increase from 15 to 20 m produced an additional 2.549 ha, equivalent to approximately 37.9% of the area inundated under the 15 m scenario (Table 3). Overall, the 20 m scenario inundated approximately 4.829 ha more land than the 10 m scenario.

The incremental map (Figure 4) shows that newly inundated areas were primarily distributed along the landward margins of the lower-scenario inundation zones. This nested expansion pattern indicates that locations close to the modeled inundation boundary are particularly sensitive to changes in the prescribed tsunami height. Areas classified as non-inundated under one scenario may therefore become inundated when a larger run-up scenario is considered.

The use of multiple scenarios is relevant because tsunami hazard is subject to substantial uncertainty associated with earthquake-source characteristics and the resulting coastal tsunami heights. Probabilistic tsunami assessments for Indonesia and at the global scale have demonstrated that uncertainties in earthquake occurrence, source characteristics, and tsunami generation can translate into considerable variability in estimated tsunami intensity and run-up (12,13). The three scenarios used here do not quantify such probabilities; rather, they provide a deterministic comparison of how the Gadingsari coastal area responds spatially to different prescribed run-up heights.

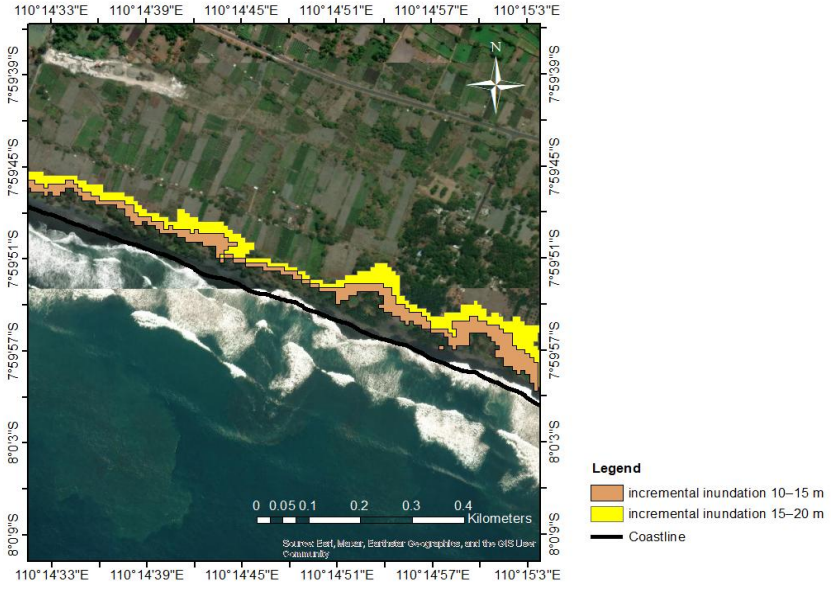


Figure 4. Incremental expansion of tsunami inundation area between different tsunami run-up scenarios.

Table 3. Additional inundation area caused by increasing tsunami run-up scenarios.

Expansion zone	Additional area (ha)
10 m–15 m	2.280
15 m–20 m	2.549

3.3. Influence of Topographic Characteristics on Tsunami Penetration

The maximum inland penetration distance increased from 82.99 m in the 10 m scenario to 134.08 m in the 20 m scenario (Table 4). This result confirms that tsunami height strongly influences the inland propagation capability of tsunami waves.

The spatial distribution of inundated cells further indicates that the modeled inundation was concentrated predominantly within elevation classes of 7.5–10 m and slope classes of 2–5°. This pattern suggests that terrain configuration contributed to the spatial variation in inland propagation. In relatively gentle terrain, less tsunami height is lost through the slope component of the attenuation model, allowing inundation to extend farther inland. Comparable GIS-based modeling at Sawarna Beach found that areas characterized by gentle slopes and low surface roughness were more susceptible to deeper inland inundation (5).

The importance of topographic representation in tsunami inundation modeling has also been demonstrated by Griffin et al. (14), who showed that differences in DEM accuracy and resolution can substantially alter modeled inundation boundaries. A study at Samas Beach in Bantul similarly found differences between tsunami modeling results produced using DEMNAS and higher-resolution UAV-derived elevation data (9). These findings indicate that the penetration distances estimated for Gadingsari should be interpreted in relation to the spatial resolution and vertical accuracy of the DEM used in the analysis, particularly where small topographic features may affect overland propagation.

Table 4. Maximum inland penetration distance under different tsunami scenarios.

Tsunami scenario	Maximum penetration distance (m)
10 m	82.99
15 m	103.99
20 m	134.08

3.4. Role of Surface Roughness in Tsunami Energy Dissipation

Surface roughness was incorporated into the model through the Manning roughness coefficient (n), which represents differences in resistance among land-use and land-cover classes. Within the Hloss formulation, the roughness contribution increases with n^2; consequently, cells assigned higher roughness coefficients produce greater modeled tsunami-height loss than smoother surfaces under otherwise similar conditions (8).

The importance of representing surface roughness in tsunami inundation models is supported by previous hydrodynamic studies. Kaiser et al. (4) demonstrated that land-cover roughness can substantially modify tsunami-flow characteristics and showed that disregarding buildings in urban areas may lead to overestimation of inundation extent. Their results also indicated a strong influence of dense vegetation on modeled flow velocity. Similarly, Griffin et al. (14) emphasized that both the representation of topography and the treatment of surface roughness affect estimates of tsunami inundation extent.

In the present study, however, the independent contribution of individual land-cover classes was not quantified separately from the effect of slope. Surface roughness should

therefore be interpreted as one component of the combined spatial resistance incorporated in the model, rather than as direct evidence that a particular land-cover type reduced inundation by a specific amount. This distinction is important because the Manning coefficients used here are model parameters representing generalized surface resistance and were not measured directly in the field.

3.5. Remaining Tsunami Height Distribution

The Remaining Tsunami Height analysis provides information regarding the residual tsunami energy after propagation and energy reduction processes. The results indicate that the distribution pattern remained relatively consistent across all scenarios, although higher tsunami scenarios generated greater remaining tsunami height values.

Table 5. Area and percentage distribution of Remaining Tsunami Height classes under 10 m, 15 m, and 20 m tsunami run-up scenarios.

Run-up scenario	Remaining Tsunami Height class (m)	Area (ha)	Percentage (%)
10 m	0–2	0.923	20.81
	2–4	0.792	17.86
	4–6	0.916	20.65
	6–8	0.785	17.70
	8–10	1.019	22.98
Total		4.436	100.00
15 m	0–3	1.385	20.62
	3–6	1.295	19.28
	6–9	1.267	18.87
	9–12	1.378	20.51
	12–15	1.391	20.72
Total		6.716	100.00
20 m	0–4	2.046	22.08
	4–8	1.853	20.00
	8–12	1.729	18.66
	12–16	2.239	24.16
	16–20	1.398	15.09
Total		9.264	100.00

For the 10 m scenario, the dominant remaining height class was 8–10 m (22.98%), while the dominant classes for the 15 m and 20 m scenarios were 12–15 m (20.72%) and 12–16 m (24.16%), respectively.

These results indicate that tsunami energy reduction is spatially variable and strongly influenced by terrain conditions and surface roughness. Areas with lower resistance maintain higher remaining tsunami height values, resulting in greater potential impacts. This spatial heterogeneity is consistent with previous studies showing that topographic representation and land-cover roughness can modify modeled tsunami inundation characteristics (3,4,14).

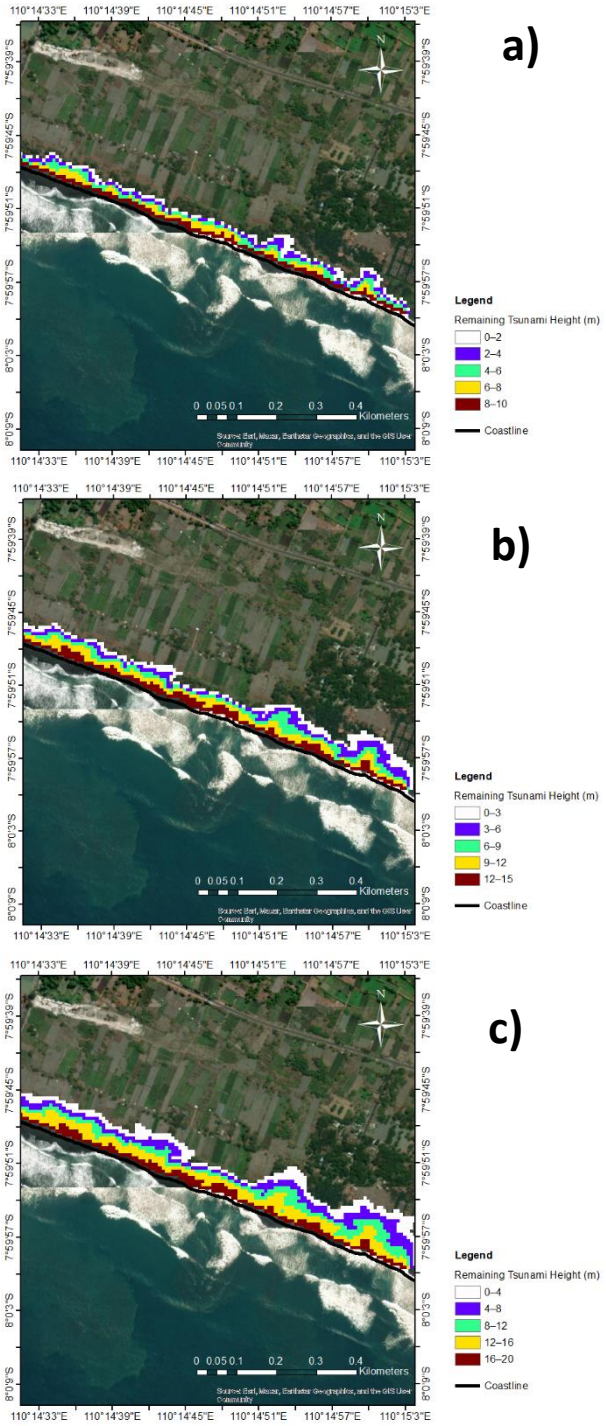


Figure 5. Spatial distribution of Remaining Tsunami Height under different tsunami run-up scenarios: (a) 10 m; (b) 15 m; and (c) 20 m

3.6. Implications for Tsunami Hazard Assessment and Mitigation

The multi-scenario analysis demonstrates that representing tsunami inundation with a single fixed boundary would not capture the range of spatial responses observed in Gadingsari. Increasing the run-up scenario from 10 to 20 m more than doubled the modeled inundation area and increased maximum inland penetration from 82.99 to 134.08 m. In particular, the incremental analysis identified transition areas along the landward inundation margins where relatively modest changes in the prescribed tsunami height resulted in changes from non-inundated to inundated conditions.

These results are relevant for first-order coastal hazard screening and evacuation planning. Tsunami inundation models can provide spatial information on potentially affected areas and identify locations that may require more conservative evacuation boundaries. Griffin et al. (14) noted that inundation-extent modeling can support first-order disaster planning, while studies in Bantul have demonstrated the application of tsunami models to exposure assessment and evacuation-route planning (7,9).

From an environmental planning perspective, the scenario-dependent expansion of inundation indicates that coastal land located near the modeled inundation margins deserves particular attention in spatial planning. Coastal vegetation, agricultural land, and other environmentally sensitive areas that remain outside the 10 m inundation zone may become exposed under the higher run-up scenarios. Maintaining appropriate coastal land use and conserving vegetated coastal zones may therefore form part of broader disaster-resilient coastal management strategies. Previous studies have highlighted the relevance of land-use management in tsunami-prone coastal areas and the potential role of coastal wetlands and vegetation in reducing inland water propagation

Nevertheless, the results should be interpreted within the limitations of the modeling approach. The present analysis uses prescribed run-up heights and a GIS-based attenuation model rather than a fully dynamic hydrodynamic simulation. It does not explicitly simulate earthquake-source dynamics, offshore tsunami propagation, time-dependent flow, velocity, or arrival time. Furthermore, quantitative validation against observed inundation data was not available. The maps therefore represent scenario-based estimates of potential inundation rather than forecasts of the exact extent of a future tsunami. More detailed hazard assessments could incorporate higher-resolution topographic data, hydrodynamic simulations, and probabilistic source characterization to evaluate uncertainty more explicitly (12-14).

Conclusions

This study demonstrates that a GIS-based multi-scenario approach can effectively characterize tsunami inundation variability in the Gadingsari coastal area, Bantul Regency. The integration of DEM, slope, land-use characteristics, and surface roughness parameters using the Hloss and Cost Distance approaches successfully generated spatial inundation patterns under different tsunami run-up scenarios. The results show that increasing tsunami height significantly expands the inundation extent, with affected areas increasing from 4.436 ha under the 10 m scenario to 6.716 ha and 9.264 ha under the 15 m and 20 m scenarios, respectively. The increase from the 10 m to 20 m scenario resulted in an additional inundated area of 4.829 ha, while the maximum inland penetration distance increased from 82.99 m to 134.08 m. The inundated areas were predominantly distributed within elevation classes of 7.5–10 m and slope classes of 2–5°, indicating that local topographic characteristics influence tsunami propagation patterns. The Remaining Tsunami Height analysis further revealed variations in residual tsunami energy distribution among different scenarios due to differences in terrain and surface resistance conditions. These findings highlight the importance of multi-scenario GIS-based tsunami modeling for evaluating coastal hazard characteristics and supporting tsunami mitigation planning. Further studies incorporating hydrodynamic simulations and quantitative validation using detailed spatial hazard datasets are recommended to improve the reliability of tsunami inundation assessments.

Conflicts of Interest

The authors declare no conflict of interest.

References

1. Purnama MR, Suppasri A, Pakoksung K, Imamura F, Farid M, Adityawan MB. Improving Indonesia's tsunami early warning: Part I: Developing synthetic tsunami scenarios and initial deployment. Ocean Engineering. 2025;316:119892. doi:10.1016/j.oceaneng.2024.119892.
2. Supendi P, Widiyantoro S, Rawlinson N, Yatimantoro T, Muhari A, Hanifa NR, et al. On the potential for megathrust earthquakes and tsunamis off the southern coast of West Java and southeast Sumatra, Indonesia. Natural Hazards. 2023;116:1315-1328. doi:10.1007/s11069-022-05696-y.
3. Amra R, Araki S, Geiß C, Davies G. Error-reduced digital elevation models and high-resolution land cover roughness in mapping tsunami exposure for low elevation coastal zones. Remote Sensing Applications: Society and Environment. 2025;37:101438. doi:10.1016/j.rsase.2024.101438.
4. Kaiser G, Scheele L, Kortenhaus A, Løvholt F, Römer H, Leschka S. The influence of land cover roughness on the results of high resolution tsunami inundation modeling. Natural Hazards and Earth System Sciences. 2011;11(9):2521-2540. doi:10.5194/nhess-11-2521-2011.
5. Arrisaldi T, Bima MAA, Nurapita KKR, Pratiknyo P. Tsunami inundation modeling and hazard mapping using GIS in Sawarna Beach, Banten Province. Dinamika Teknik Sipil: Majalah Ilmiah Teknik Sipil. 2025;18(1):11-19. doi:10.23917/dts.v18i1.10617.
6. Kimpton T, Higuera P, Whittaker C, Wotherspoon L, Zorn C. A rapid simplified method for determining tsunami inundation extent based on energy conservation. Computer-Aided Civil and Infrastructure Engineering. 2024;39(12):1811-1829. doi:10.1111/mice.13168.
7. Budiman MJ, Sutoyo, Syafiudin MF. Pemetaan kerentanan bahaya tsunami dengan pemodelan inundansi (studi kasus: Kabupaten Bantul). Jurnal Teknik Sipil dan Lingkungan. 2024;9(2):157-166. doi:10.29244/jsil.9.2.157-166.
8. Berryman K. Review of Tsunami Hazard and Risk in New Zealand. Wellington: Institute of Geological & Nuclear Sciences; 2005. Client Report 2005/104.
9. Sihombing S, Sudarmaji, Sunardi B, Darmawan H. Tsunami modeling using DEMNAS and DEM data from UAV surveys for planning evacuation routes on Samas Coast, Bantul Regency. Journal of Geoscience, Engineering, Environment, and Technology. 2024;9(2):152-157. doi:10.25299/jgeet.2024.9.2.14777.
10. Badan Informasi Geospasial. DEMNAS/DEM_Indonesia (ImageServer). BIG Geospatial Services. https://geoservices.big.go.id/raster/rest/services/DEMNAS/DEM_Indonesia/ImageServer. Accessed 2026 Oct 6.
11. Badan Informasi Geospasial. Ina-Geoportal. https://tanahair.indonesia.go.id/portal-web/webmap. Accessed 2026 Oct 6.
12. Horspool N, Pranantyo I, Griffin J, Latief H, Natawidjaja DH, Kongko W, et al. A probabilistic tsunami hazard assessment for Indonesia. Natural Hazards and Earth System Sciences. 2014;14:3105-3122. doi:10.5194/nhess-14-3105-2014.

13. Davies G, Griffin J, Løvholt F, Glimsdal S, Harbitz C, Thio HK, et al. A global probabilistic tsunami hazard assessment from earthquake sources. Geological Society, London, Special Publications. 2017;456:219-244. doi:10.1144/SP456.5.
14. Griffin J, Latief H, Kongko W, Harig S, Horspool N, Hanung R, et al. An evaluation of onshore digital elevation models for modeling tsunami inundation zones. Frontiers in Earth Science. 2015;3:32. doi:10.3389/feart.2015.00032.

CC BY-SA 4.0 (Attribution-ShareAlike 4.0 International).
This license allows users to share and adapt an article, even commercially, as long as appropriate credit is given and the distribution of derivative works is under the same license as the original. That is, this license lets others copy, distribute, modify and reproduce the Article, provided the original source and Authors are credited under the same license as the original.

